Microfabrication of High-Frequency Vacuum Electron Devices

R. Lawrence Ives, *Senior Member, IEEE*

***Abstract*—Advances in manufacturing technology for microstructures are allowing new opportunities for vacuum electron devices producing radio-frequency (RF) radiation. Specifically, the capability to produce small circuit structures is allowing development of RF devices at frequencies impractical with traditional machining technology. This is generating increased interest in applications in the submillimeter and terahertz frequency range. High-power RF devices in this frequency range are needed for medical, communications, defense, and homeland security applications. This paper describes the most promising microfabrication techniques applicable to high-frequency RF devices and examples of recent applications.**

***Index Terms*—Backward wave oscillator (BWO), cold cathode, deep reactive ion etching (DRIE), electrical discharge machining (EDM), field emission, field emitter array (FEA), focused ion beam (FIB), LIGA, radiation, RF source, spectroscopy, SU-8.**

I. Introduction

ADVANCES in microfabrication technology are providing new opportunities for vacuum electron devices (VEDs) producing radio-frequency (RF) power in the millimeter and submillimeter frequency range. Until recently, production of compact VED-based RF devices was typically limited to frequencies below 100 GHz. As operating frequencies approach 100 GHz, the ability to achieve the required machining tolerances becomes problematic, even with the most advanced computer controlled milling machines and lathes. Manual assembly, including brazing and welding, also becomes impractical. Traditional production procedures become difficult when parts can be seen only with a microscope.

This is a new area for those of us who began our careers working with S band klystrons or 100-kW gyrotrons. We could not lift those devices because they were too heavy; now we're working with devices that break if we touch them. It's a new world for high-frequency RF designers, but one with a tremendous potential. The submillimeter and terahertz (THz) regions are areas where electron mobility in semiconductors cannot meet the specifications, but electrons traveling in vacuum can, assuming the electric and magnetic fields can be shaped to modulate the beams and convert their energy to RF power.

The potential applications are impressive. The Department of Defense has ranked the early-warning detection of chemical and biological agents at highest priority [1]. Significant research is in progress to develop techniques for remote sensing of these agents for protection of troops in the field, as well as highly populated areas, such as airports, train stations, ball parks, and public buildings. A technology that is demonstrating particular advantages for this purpose is terahertz radiation, sometimes referred to as T-rays. There is an abundance of molecular rotational energy levels of free molecules in this frequency range that can be used to identify specific molecules and materials. DNA, for example, possesses unique resonances in this frequency range due to localized phonon modes, providing a means for identifying biological agents [1]. Recent experiments demonstrated use of terahertz radiation to identify various powder substances in envelopes, including flour, salt, baking soda, and Bacillus thruengiensis bacteria [2].

Detection of chemical and biological agents using terahertz radiation is particularly attractive in areas where people are present. The photon energy of terahertz radiation is a million times less than that of X-rays and produces no biological tissue damage [3]. T-rays also easily penetrate most dielectrics, including paper, cardboard, clothes, luggage containers (nonmetallic), wood, and many building materials. Terahertz radiation can not only provide spectroscopic information; it can also produce high-resolution images of metallic objects. A security system using terahertz radiation could be placed in large, highly populated areas, such as train stations, airports, subway/train stations, and building entrances to image hidden weapons and respond to spectroscopic signatures of explosives, biological and chemical agents, and other dangerous substances. The system would be completely harmless to animals and plants.

Unfortunately, there are no economical, high average power sources of terahertz radiation. Two techniques are currently used for experimental studies [4]. Both methods use ultrafast pulses of laser radiation. A typical source is an ultrafast Ti : sapphire laser with an average power of 1 W delivering 100-fs pulses at 800 nm. In the photoconductive approach, high-speed photoconductors serve as transient current sources for radiating antennas. Typical conversion efficiency of the optical power to terahertz radiation is 10^{-3} to 10^{-6}. The second approach uses electrooptic crystals to provide optical rectification. Conversion efficiency is from 10^{-4} to 10^{-6}. Output power for these approaches is from 0.1 to 100 mW. For a two-dimensional (2-D) imaging system, average powers of milliwatts or higher would be required for a practical device with sufficient response [4]. Using the existing technology, for example, it requires approximately 8 min to scan an envelope [2]. This obviously would be too slow for remote sensing of large, public areas or large quantities of containers or packages.

In addition, the laser-based systems are large and expensive. Current systems require a few square meters, and imaging sys-

Manuscript received September 12, 2003; revised December 8, 2003.

The author is with Calabasas Creek Research, Inc., Saratoga, CA 95070-3753 USA (e-mail: rlives@calcreek.com).

Digital Object Identifier 10.1109/TPS.2004.827595

0093-3813/04$20.00 © 2004 IEEE

tems cost approximately \$200 000 [4]. Most of the size and expense is for the ultrafast laser.

Larger system bandwidths are available with the higher frequency bands, enabling high data rate communications competitive with optical technology. For example, assuming a 5-GHz bandwidth and 5-bits/s/Hz bandwidth efficient modulation scheme, data rates of approximately 25 Gb/s can be achieved for a W band traveling wave tube (TWT). Using carrier frequencies above 300 GHz, oscillator and amplifier sources with $\sim 10\%$ fractional bandwidths would enable very high data rate ($>$ 10 Gb/s) wireless communications with high security protection [5]. If adequately powerful, compact, and wide-band sources were available, this capability could be realized with extremely simple, low-cost, amplitude modulation schemes (for example, simple amplitude modulation and diode receivers). The critical roadblock to full exploitation of the THz band is lack of coherent radiation sources that are powerful (0.01 to 10.0 W CW), efficient (1%), frequency agile (instantaneous fractional bandwidths $>1\%$), reliable, compact, and affordable.

Compact high-frequency amplifiers would also be ideal for airborne synthetic aperture radar (SAR), providing ground reconnaissance through clouds and weather, and ground moving target indicator capabilities. Microelectromechanical systems (MEMS)-based TWTs are particularly appropriate for the extremely limited payload capacity on unmanned aerial vehicles. Inverse SARs, which use Doppler shifts from an object's motion to create images of the object, also require compact amplifier technology. These are particularly useful for maritime surveillance, where swaying of ships at sea allows precise identification from known superstructures [6].

The U.S. Army is funding a program to investigate MEMS-based, Ka band TWTs producing about 10 W of RF power. These devices would potentially be used as RF sources for phased array antennas. Consistent with the Army's vision of a network-centric force, the TWTs would aid in networking a large number of army units by enabling high data rate transmission. This would include communications, radar, and combat identification. Because of the application to phased arrays, a large number of compact TWTs are required. This will require innovative TWT designs, which result in improved repeatability, increased yields and reliability, and reduced cost over existing Ka band devices. In addition, the devices must be scalable in frequency for higher frequency operation and include field emitter array (FEA) technology [7].

The July 28, 2003 edition of *U.S. News and World Report* described some potential applications of terahertz radiation for medical purposes. An important application is medical imaging. Terahertz radiation is quickly absorbed by water and similar fluids making them adept at picking healthy cells from cancerous cells because of the difference in blood flow. Addenbrooke's Hospital in Cambridge, U.K., is bouncing terahertz radiation off cells and distinguishing skin cancer from healthy tissue. Unlike X-rays, which can only detect tooth decay at later stages, terahertz radiation could detect the first stages of demineralization, allowing noninvasive treatments such as fluoride rinses.

As economical high-frequency RF sources become more available, additional applications will undoubtedly be developed. Microfabrication techniques must provide the necessary capability to develop these sources. This paper will briefly describe the principle techniques currently being investigated for the production of high-frequency vacuum electron devices. As a tube designer and builder, I claim no special expertise in these techniques, but attempt only to describe the basic processes and present references for further investigation by interested readers. All this research is ongoing and progressing rapidly, so readers should consult the current literature for the latest information.

I am also approaching this topic as someone responsible for building and delivering working products. Our company performs advanced research and development of high power sources and components. Our customers expect working prototypes by the end of our programs, so we are not in the business of implementing processes or procedures that do not result in real devices. Consequently, we are concerned with mechanical and electrical characteristics, braze ability, operation in typical VED environments, handling, ability to survive baking, ruggedness, reliability, reproducibility, and finally cost. As will be seen, most of the microfabrication options today are not sufficiently mature to implement in deliverable devices, but it will take cooperative research involving those involved in process development and those involved in VED development to bridge the gap between laboratory capability and production devices. Hopefully, information provided here will help in that effort.

Section II will provide basic information on microfabrication techniques under investigation for VED development. Some examples of work in progress will be provided. Section III will describe a number of development programs utilizing some of these techniques to build real structures, such as electron guns, RF circuits, and waveguides and windows. Section IV describes additional microfabrication research and development that will be required to transition these techniques into a production environment, and Section V will provide a brief summary on the current state of microfabrication of high-frequency vacuum electron devices.

II. Microfabrication Techniques

This section will describe the most promising microfabrication techniques for producing components and structures for millimeter and submillimeter RF devices. It does not include all microfabrication techniques that might be applicable, but does include all those known to the author that are currently being used to produce experimental VED structures.

A. LIGA

LIGA is an abbreviation of *Lithographe, Galvonoformung, und Abfornung* and translates as lithography, electroplating, and micro-molding. The process uses X-rays from a synchrotron to expose a resist material through a metallic mask containing an image of the structure to be produced. The basic process is illustrated in Fig. 1 [8]. Poly-methylmethacrylate (PMMA) is deposited on a metal substrate up to a maximum thickness of ap-

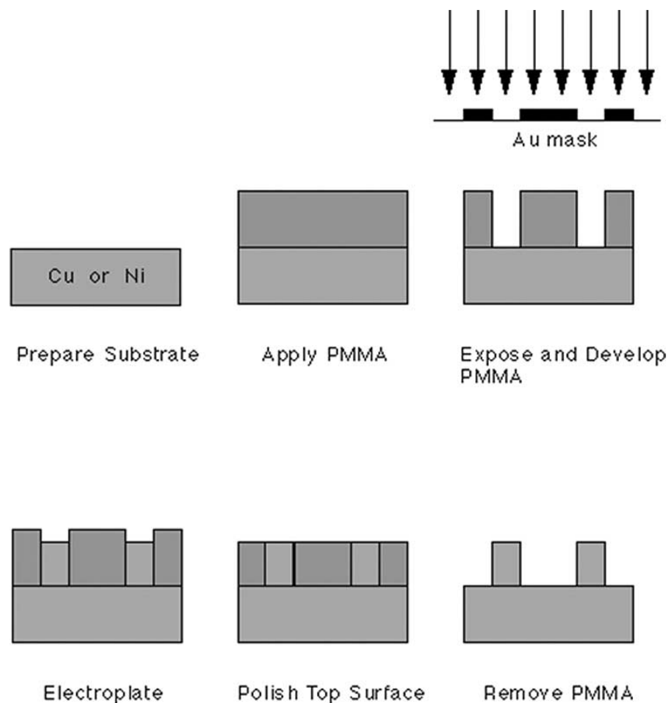

Fig. 1. Basic process for creating microstructures using LIGA.

proximately 1 mm. In some cases, a thin titanium coating is applied to the metal substrate before deposition to improve adhesion. Following deposition (casting) it is annealed at temperatures between 110 °C and 170 °C. An X-ray mask containing the image of the desired part is placed over the PMMA, and the structure is exposed to X-rays produced by a synchrotron. Only synchrotrons can provide the dose rates required, approximately 3000–10 000 $\mathrm{J/cm^3}$, and several hours of exposure are required [9]. Following exposure, regions of the PMMA impacted by the X-rays are removed, leaving a positive image. The removed regions are replaced by electrodeposited metal, and the structure is lapped to the desired thickness. The remaining PMMA is removed to obtain the finished part.

In practice, the process is a bit more complicated. Considerable care is required in the creation of the exposure mask. In the process reported by Nassiri *et al.*, an optical lithographic mask was used to create a high-contrast X-ray projection mask [10]. This, in turn, was used to generate a high accuracy mask using soft X-rays.

Adhesion of the PMMA is also an issue. Researchers at Argonne National Laboratory required a roughness of less than 0.1 μm [11]. They finished copper substrates with diamond polishing to achieve a flatness of 1 μm over 4 in. Then either an oxide film was grown to 1 μm thickness or an equally thick titanium coating was applied. At Sandia National Laboratory, a titanium coating is applied. Still, there can be problems, and a part being manufactured for the author was lost when the PMMA prematurely released from the substrate. Different solvents are

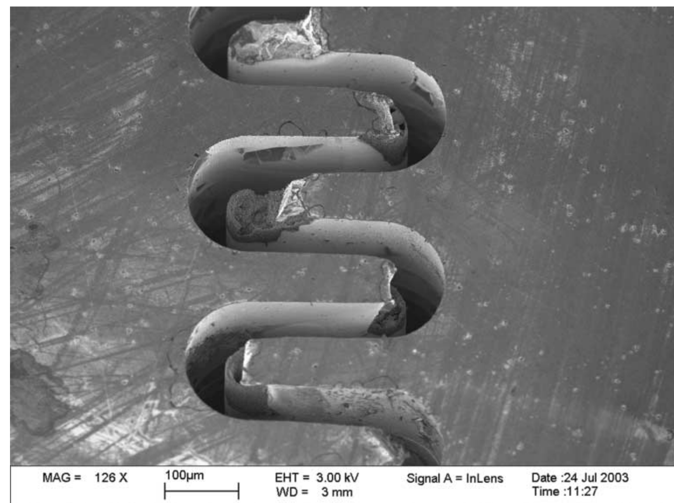

Fig. 2. Results of recent attempt to produce a folded waveguide circuit using LIGA.

available for removing PMMA exposed to the synchrotron radiation.

Material is electroplated in the regions where PMMA was removed, and the structure finished to the desired thickness. A number of materials can be electroplated, including nickel, copper, gold, tin, lead, and iron, as well as various alloys, including NiP, NiCo, NiFe, and brass [12]. More recent development allows electroplating with nonaqueous or aprotic electrolytes. This allows electroplating of aluminum, some ceramics, electrically conductive polymers such as polypyrrole and electrophoretic deposition of ceramic nanoparticles.

LIGA successfully produced precision parts for a number of RF related devices, including a 32-cell, 108-GHz constant impedance cavity at Argonne National Laboratory [11], [13], muffin-tin accelerator structures at 94 GHz [10] and 91.4 GHz [14], and a circuit for a 10-kW, W band klystrino [8]. This is not a production process, however. Efforts by the author to obtain circuits for a terahertz backward wave oscillator (BWO) required approximately 18 months of development. Recent attempts by a commercial vendor to manufacture a folded waveguide circuit for the University of Wisconsin resulted in the part shown in Fig. 2, which was delivered many months after order placement [15]. Previous efforts at Argonne National Laboratories were more successful, indicating that, while this process is viable in a research environment, it has not yet transitioned to a commercial process.

When LIGA works, it can produce some impressive results. Fig. 3 shows a close-up of pintles constituting part of a 600–700 GHz BWO circuit. The copper pintles are 20 μm in diameter and 80 μm high. The spacing between pintles is 30 μm in one direction and 34 μm in the other. Note the fine surface finish and uniformity in the features. There are 1500 of these structures that make up the entire circuit. It should be noted, however, that of the 50 circuits on the wafer containing this circuit, only four were successfully produced.

A fundamental problem with LIGA, however, is the requirement for a synchrotron. The investment in a LIGA-capable X-ray source is more than $20 million without building and beamlines [16]. The total cost for a reasonably equipped LIGA

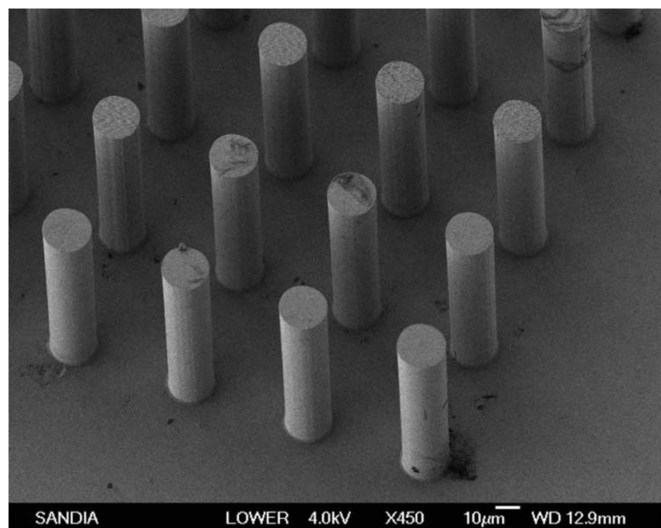

Fig. 3. Close-up of copper pintles of a 600–700 GHz BWO circuit.

lithographic facility is more than $40 million. Availability of existing facilities is becoming seriously impacted by research and medical applications. It is questionable whether facilities will be available for commercial and production applications in the next few years.

B. SU-8

SU-8 is a lithographic process using a negative photoresist originally developed by IBM [17]. It consists of a polymeric epoxy resin dissolved in an organic solvent together with a photoacid generator [19]. The SU-8 is placed on a silicon wafer to the desired thickness. It can be spun up to a thickness approaching 500 μm in a single step [9]. Multistep applications can achieve thicknesses greater than 1 mm. Thickness nonuniformity will result in exposure nonuniformity in later processes as will any tilting of the substrate. The wafer is then baked at a low temperature to remove the solvent. In the procedure used by Jingquan *et al.*, the wafer is initially baked at 65 °C for 10 min, then at 95 °C for 1 h. The initial bake is designed to keep the internal stresses in the material low. Lian *et al.* report using a 240 °C bake for 240 min for a 500 μm thickness of SU-8 [19]. Singleton *et al.* reports using a 45-min bake at 250 °C–275 °C in a vacuum oven for a 505–510 μm thickness [20].

SU-8 has low optical absorption in the ultraviolet (UV) range at 365-nm wavelength, so the photoresist film can be used with thicknesses greater than 1 mm. When exposed to UV light, absorption of a photon reacts with the photoacid generator to form a photoacid acting as a catalyst. This photoacid causes a crosslinking reaction, primarily during a post exposure bake (PEB). Crosslinking only occurs where the photoacid is present; i.e., in regions exposed to UV radiation. The PEB completes the crosslinking reaction and varies between researchers. The degree of crosslinking depends on both the exposure dose and bake conditions. Singleton *et al.* perform an intermediate bake at 50 °C for 5 min, followed by a 90 °C bake for 15 min. After PEB, the resist was developed with a two stage process using a solvent, followed by an isoproponal wash and air dry.

An alternative to UV exposure of SU-8 utilizes X-rays from a synchrotron [20], [9]. The process is similar to LIGA except the dose required is significantly less. LIGA exposure requires several hours to achieve a total dose on the order of 4000 $\mathrm{J/cm^3}$. Typical dose for SU-8 is only 30 $\mathrm{J/cm^3}$.

Impressive structures can be found in the literature; however, there are a number of significant problems with SU-8 lithography. Performance is very sensitive to the process parameters. All parameters, including resist deposition, pre-exposure bake, exposure dose, post exposure bake, and final development, impact the performance.

There are also a number of different formulations of the material, each one displaying different properties. Many of the studies reported in the literature are focused on determining optimum parameters for various applications. A common problem appears to be internal stresses in the resist. Such stresses can result in cracked lithographic features and may be a potential limitation for device fabrication [21]. Other reported issues include solvent removal before exposure, substrate adhesion, photoacid mobility, image transfer during exposure, mask sticking, degree of crosslinking, and temperature instability of the resist.

C. Deep Reactive Ion Etching

Deep reactive ion etching (DRIE) is a process where high-aspect ratio structures are etched into silicon. These structures can be used to generate molds or serve as a mold itself for generating metallic structures. Silicon structures ranging from two to hundreds of micrometers can be created. Fluorine based chemistry is typically used because of its high etch rate (10 μm/min) and selectivity (100 : 1) [22]. The silicon is etched with SF_6. Anisotropy is improved by ion impact assistance coupled with sidewall passivation using flourocarbon polymer deposition and/or O_2 plasma oxidation and redeposition at the silicon sidewall surface. The flourocarbon polymer consists of a chain of CF_2 molecules similar to Teflon with a film thickness of approximately 10–50 nm. It is derived from a 4–8 s application of C_4F_8 applied as a plasma source gas. The introduction of O_2 improves anisotropy by acting as a gettering agent for carbon [23]. The following etch cycle consists of 4–12 s of SF_6, applied as a plasma source gas. The ion assisted SF_6 removes the polymer passivation on horizontal surfaces prior to etching the underlying the silicon, leaving the polymer on the sidewalls relatively intact. The basic process, as described by O'Brien *et al.*, is illustrated in Fig. 4 [22]. Scalloping occurs when the reactive fluorine contacts nonpassivated silicon and is more pronounced near the top of the structure.

Significant variables include etch cycle time, passivation cycle time, and RF coil power. O'Brien *et al.* reported the impact to these parameters on etch performance in [22]. There appears to be two manufacturers of equipment for DRIE, Alcatel and Surface Technology Systems. Micromachined structures in silicon are often categorized as bulk or surface techniques. Bulk micromachined devices include pressure and acceleration sensors, most microvalves, and micropumps [24]. Thicknesses can range from 100 to 600 μm and usually include the silicon substrate as an active element in the device. Surface devices include micromotors, polysilicon-based accelerometers, micromirror devices [25], polysilicon and fusion-bonded

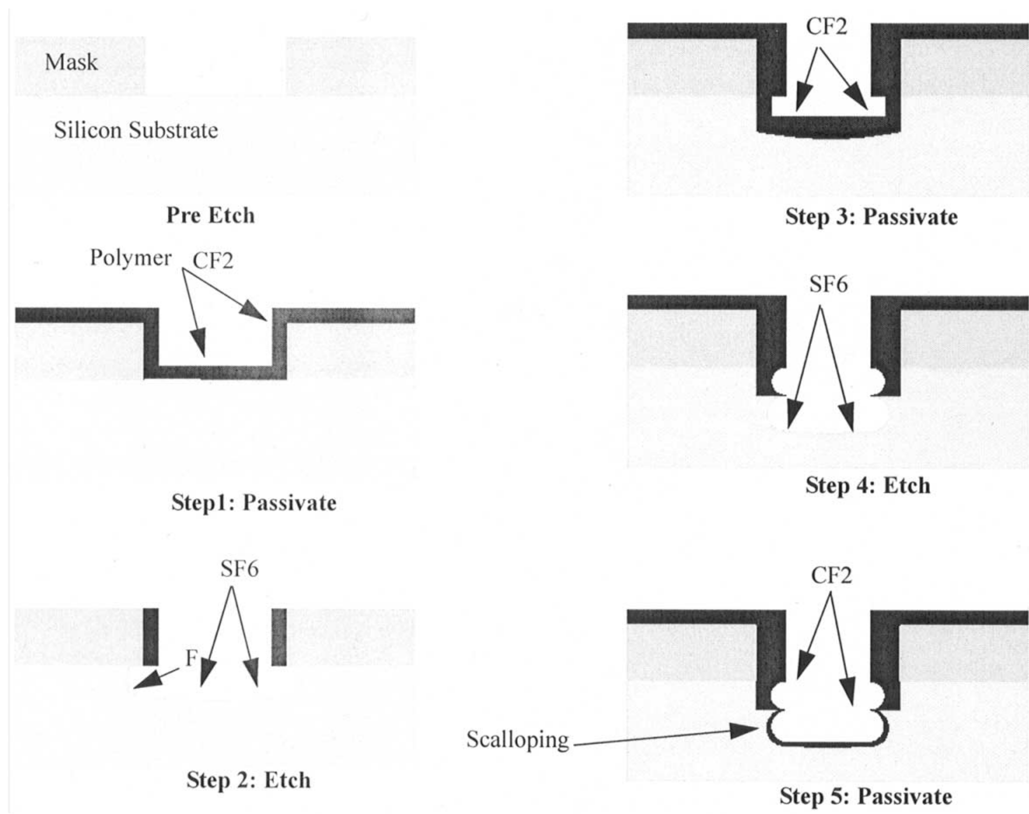

Fig. 4. Illustration of deep reactive ion etching of silicon.

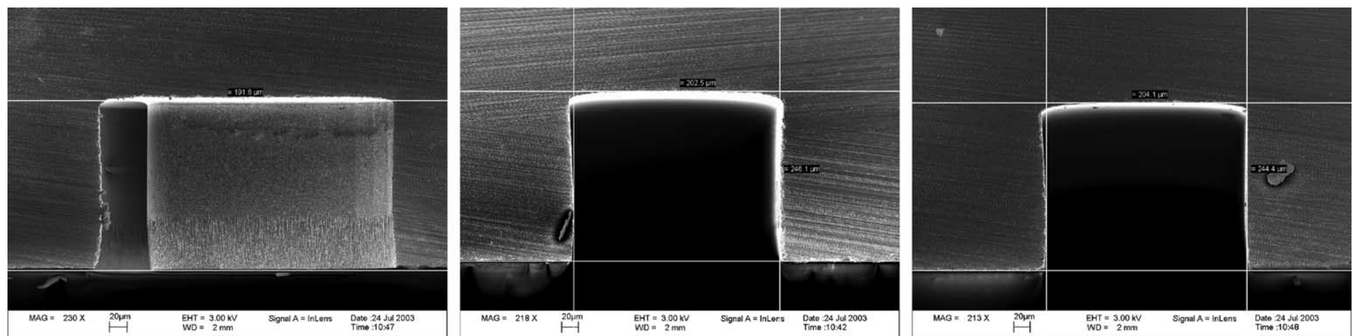

Fig. 5. SEM views of serpentine folded waveguide circuit for a submillimeter traveling wave tube. The trench width of the left image is approximately 30 μm wide and 190 μm deep. The depth of the center and right trenches is approximately 246 μm with a width of 203 μm.

resonant structures, and dissolved wafer structures. In these devices, the silicon substrate only serves as a support, and the thickness of the structures is typically several micrometers.

Fig. 5 shows scanning electron microscope (SEM) photographs of cross sections of a folded waveguide circuit for a submillimeter traveling wave tube under development by Booske *et al.* at the University of Wisconsin-Madison [26]. An issue is the straightness of the sidewalls which could cause release problems if the structure is used as a mold. Another issue is the scalloping that occurs as a result of the cycling between passivation and etching. These features can be significant when working at high frequencies. Recent work by Booske *et al.* may be reducing the significance of this characteristic.

D. Electrical Discharge Machining

Electrical discharge machining (EDM) is a precision metal removal process that uses thermal energy from a fine, accurately controlled, electrical discharge to erode material from a conductive substrate [27]–[29]. In wire EDM, a thin, energized wire produces the spark required to erode the workpiece. A dielectric fluid, typically deionized water, is forced between the wire and workpiece to prevent a short circuit. The intense, but extremely localized, heat from the arc boils off microscopic bits of the workpiece with thousands of pulses per second. The wire is continually fed through the workpiece by a wire drive unit. Important parameters include the nature of the wire, wire tension, workpiece material, arc energy, arc frequency, pressure of dielectric fluid, and wire feed rate. The wire is typically 0.15–3.0 mm nickel coated brass, copper–tungsten, or graphite. Wire as small as 20 μm is currently in use for precision machining [30], [31].

Because EDM erodes metal with electrical discharges, the hardness of the workpiece does not determine machinability of the material. A relatively soft graphite or metallic electrode can

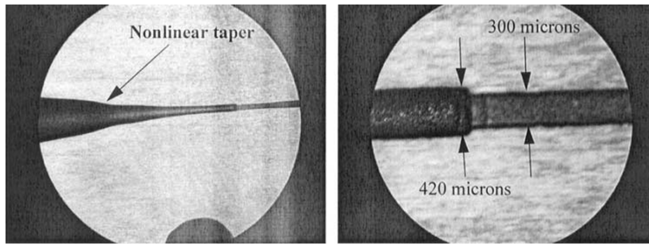

Fig. 6. Sections of 650-GHz waveguide step transformer and optical mode launcher. The dimensions of the waveguide on the extreme right are 30×300 μm. The transformer contains steps of approximately 50 μm in both dimensions. The left section contains a cylindrical, nonlinear mode converter designed with a computer optimization program.

machine hardened steels or tungsten carbide. Workpieces can be machined after heat treating, which eliminates the risk of damage or distortion during heat treating.

In sinker or plunge EDM, an electrode is used to produce the spark. The electrode is shaped depending on the geometry of the final piece. During operation, the electrode moves toward the workpiece until the space between them is such that the electric field ionizes the dielectric fluid between them, creating an arc. The fluid is typically a dielectric oil. A typical pulse rate is 250 000 times per second, and the amount of material removed depends on the energy of the pulse. The molten metal is cooled by the dielectric fluid and flushed away with the fluid.

Plunge EDM can produce complex three-dimensional (3-D) structures. Fig. 6 shows a section of a step transformer and mode converter for a 600–700 GHz backward wave oscillator. The input rectangular waveguide on the right is 30×300 μm. There are a series of waveguide steps of approximately 50 μm in both the depth and height of the waveguide. The final section is a cylindrical, nonlinear, tapered, mode converter designed using a computer optimization program in CASCADE [32]. The negative image of the nonlinear taper was incorporated into an electrode using wire EDM, which was then used to generate the 3-D structure. This device was built and successfully tested at NASA's Jet Propulsion Laboratory.

In addition to plunge and wire EDM, there are also electrical discharge milling, electrical discharge grinding, electrical discharge dressing, double rotating electrodes EDM, and mole EDM [29]. Mole EDM can create a curved path or tunnel through a workpiece.

There are several advantages of EDM over lithographic techniques. As demonstrated in Fig. 6, 3-D structures can be manufactured, whereas lithographic techniques only produce 2-D planar structures. EDM also starts with forged metals, whereas lithographic processes typically rely on electroplated metals. There are concerns about the mechanical characteristics of electroplated metals, particularly with regard to high-temperature brazing or baking.

EDM machines can be quite expensive, on the order of several hundred thousand dollars. Setup can be quite tedious also, so there could be significant labor costs. Once programmed, however, the machines can generate the most complicated parts in a few days. For large quantity production, one has to balance the fabrication time per part with the long lead times typically incurred with lithographic approaches.

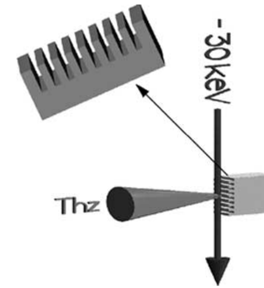

Fig. 7. Smith–Purcell based tunable terahertz source.

E. Electrochemical Milling

Electrochemical milling is similar to plunge EDM, except that ultrashort voltage pulses are applied in the presence of a static or low frequency potential in an electrolytic bath [33]. The dissolution process is sharply confined to the region of the smallest gap between the tool and the workpiece by nano- or picosecond pulses. Upon application of the short pulse on the tool, the polarization of the electrolyte double layer at the surface of the work piece rises with a time constant given by the capacitance and length of the arc path across the gap acting as the charging resistor. The electric potential required for dissolution occurs only in regions where the working gap is smaller than a well-defined minimum width, depending on the pulse duration. Using suitable electrolytes and electrical parameters, a variety of materials can be machined at submicrometer gap width without any detectable wear of the tool or thermal damage to the work piece. Gmelin *et al.* reported reproducing approximately 25-μm diameter holes to an accuracy of 100–200 nm. They produced 5-μm diameter holes greater than 1 mm deep using a machine capable of producing 1000-A 500-ps pulses.

F. Dicing

Dicing uses a diamond saw to cut very thin slots or trenches. This technique is commonly used in the semiconductor industry to cut silicon wafers. The process can cut hard, brittle materials, including ceramics, hardened copper, ferrites, molybdenum, quartz, sapphire, and tungsten [34]. Dicing works for slot features down to about 25 μm wide by 100 μm deep [35]. It is possible that dicing techniques could be applied to silicon substrates and followed by some form of electroplating or other coating to produce a conductive surface.

An advantage of the dicing technique is its cost for one of a kind or prototype production. Since the setup and tooling costs are minimal, one can explore more possibilities to optimize power and efficacy of the device. A disadvantage is that it is difficult to maintain good control of dimensions and finish of the slots and requires an experienced and patient technician to perform the dicing.

Mross *et al.* at Vermont Photonics, Inc. used dicing in the development of a tunable terahertz radiation source based on John Walsh's Smith–Purcell laser [36], [37]. The basic configuration is shown in Fig. 7 and uses a grating with 100-μm-deep slots that are 25 μm wide. A 28–34 kV electron beam passes over the grating to produce pulsed or CW RF power. Two prototype tunable sources are currently producing microwatts of tunable,

narrow-band output from 0.3 to almost 2 THz. The principle application is high-resolution terahertz spectroscopy.

G. Focused Ion Beam Milling

Focused ion beam (FIB) milling is available for inserting interconnects in semiconductor devices. Initially, interconnects were primarily aluminum; however, higher performance is available using copper. The ion beam, typically Gallium, scans the surface to be milled at low power to create an image or map of the surface [39]. For etching aluminum, the ion beam energy is increased and a halogen gas (bromine, chlorine, or iodine) is directed at the impact point. The ions induce a chemical reaction that selectively etches the target material. For copper, however, the halogens react with copper to create nonvolatile copper halides that are both electrically conductive and corrosive. Milling copper without the halogen leads to formation of a Cu_3Ga phase that inhibits etching and contributes to uneven trench profiles. In a process developed by Casey *et al.* and called CopperRx, smooth wall trenches are generated without creation of corrosive by-products [40]. In this process, an "egg crate" pattern is milled into the copper surface to inhibit lateral propagation of the Cu_3Ga phase. This pattern also provides increased surface area that is not perpendicular to the incident beam, resulting in more efficient milling. The egg crate pattern is milled while flowing $W(CO)_6$ gas over the surface, which further reduces Cu_3Ga formation. The region is subsequently milled using normal FIB milling without any gas present. Over etch is typically limited to 0.1–0.2 μm.

The author is not aware of applications of this technique to RF devices. Examples in the references cited describe trenches less than 5 μm deep. Li *et al.* reported FIB milling of nano-scale grating structures for strain gauges [41] consisting of 80-nm trenches cut into poly-Si. A similar pattern in copper could serve as a slow wave structure for a terahertz frequency RF source. The process appears more applicable to nanoscale structures than microscale devices; however, this is a relatively new technology, and additional capabilities are certain to evolve.

H. Other

Microstructures are produced by other techniques, including electron beam etching and laser etching/drilling. The author is not aware of use of these techniques to produce VED-related components; however, these and other techniques are undergoing rapid development. Interested readers should continue to follow the literature to determine if these might become appropriate for RF-related devices.

III. Microfabrication of VED Components

A. Cathodes and Electron Guns

All vacuum electron devices require a high-quality electron beam to generate RF power. Traditionally, VED employed thermionic cathodes operated at temperatures between 850 °C and 1000 °C, depending on cathode type. Lithographic microfabrication has now been applied to produce field emission array cathodes that operate at room temperature and can, in special cases, produce current emission densities in excess of several 100 A/cm^2. There are problems, however, that have prevented their use in production RF devices. Research is underway to study these issues and attempt to develop practical solutions.

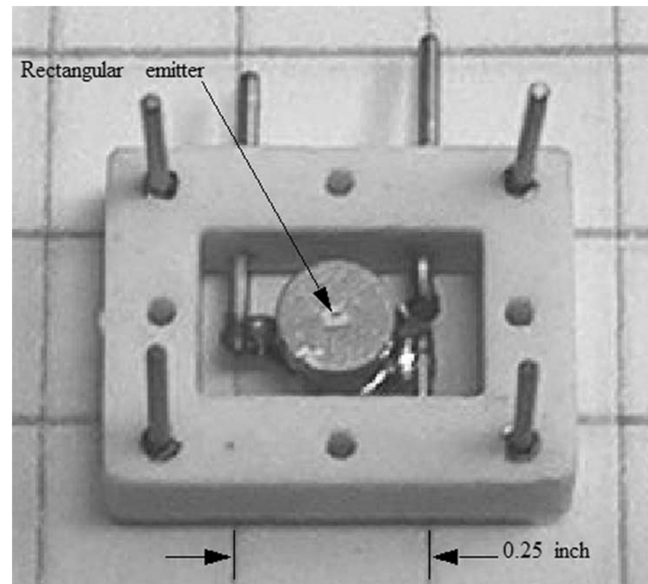

Fig. 8. Istok cathode producing 125 A/cm^2 in a 100×300 μm rectangular beam.

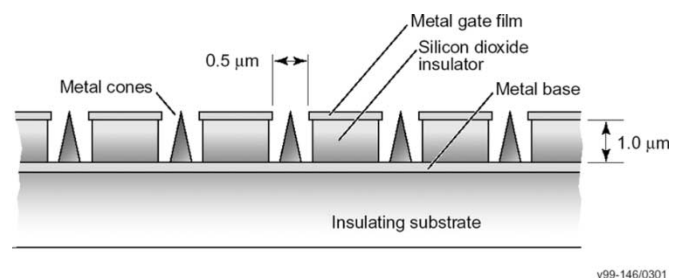

Fig. 9. Schematic configuration of the Spindt FEA. (Reproduced from *Vacuum Microelectronics*, W. Zhu, Ed. New York: Wiley, 2000).

As the frequency or RF devices increase, the circuit size, and, consequently, the beam size decreases. It becomes more difficult to obtain large beam compressions in microfabricated devices, so it is advantageous to develop cathodes that can operate at high current density.

The highest current density thermionic cathodes that the author is aware of are manufactured by Istok Company in Russia. These cathodes are used in submillimeter wave backward wave oscillators and produce approximately 125 A/cm^2; however, they operate at 1200 °C. One of these cathodes is shown in Fig. 8. The cathode surface is coated with a nonemissive material except for a 100×300 μm area in the center. The BWO uses a rectangular electron beam.

A BWO utilizing one of these cathodes has been in operation at the Jet Propulsion Laboratory for several years, though the total number of hours of operation are unknown. Operation of cathodes at 1200 °C would imply a very limited lifetime. Calabazas Creek Research, Inc. (CCR) is currently installing one of the Istok cathodes in a 600–700 GHz BWO under development for the National Aeronautics and Space Administration

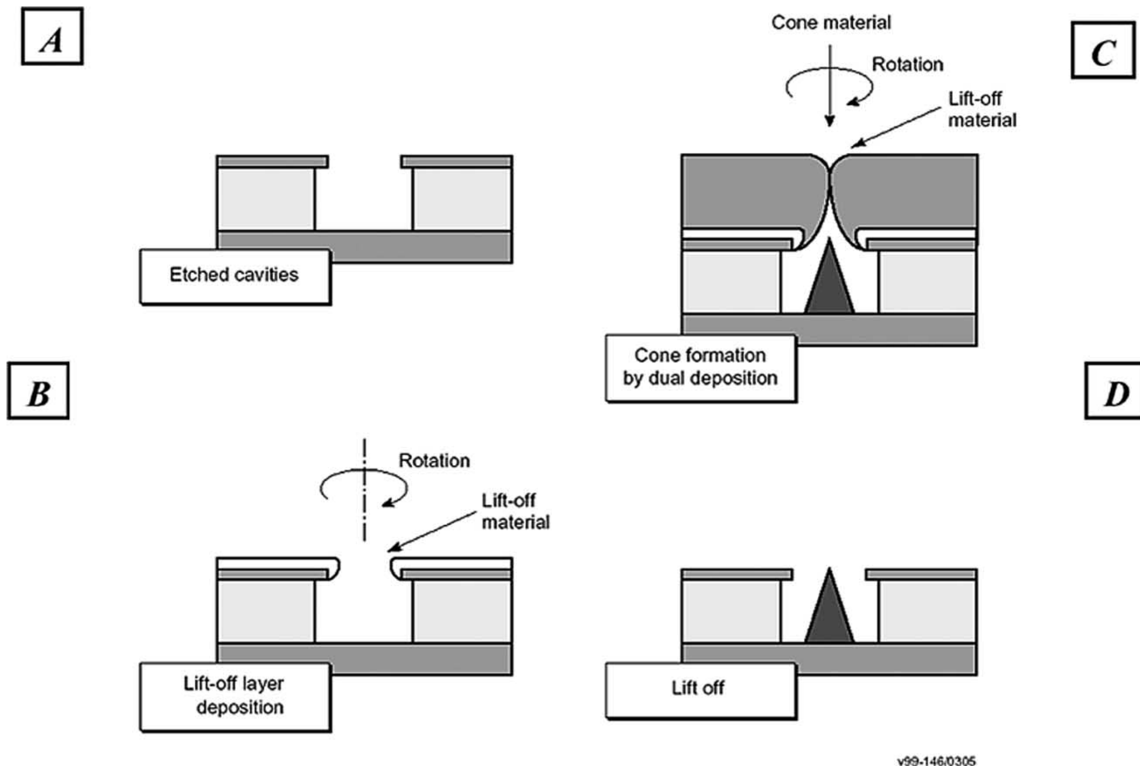

Fig. 10. In the simplified fabrication process, cavities are etched in the top two layers of a metal/dielectric material/ metal stack using resist patterning and wet or dry etching. A sacrificial liftoff layer (b) is deposited on the top layer while rotating the substrate. Cones are formed in the cavities (c) by depositing metal perpendicular to the substrate surface. The precise configuration can be controlled using grazing angle deposition to control hole closure and manage stresses in the deposited layer. Liftoff (d) is performed with a wet etch using a solvent that only attacks the liftoff material. (Reproduced from *Vacuum Microelectronics*, W. Zhu, Ed. New York: Wiley, 2000).

(NASA). This BWO will be described in more detail in Section IV. CCR was also funded by NASA to develop such cathodes as part of its BWO development program.

Field emission array cathodes offer significant advantages for high-frequency RF sources, providing problems can be overcome. FEAs are produced lithographically and have demonstrated emission current densities well in excess of 500 $\mathrm{A/cm^2}$ in laboratory environments for small arrays. A proposed FEA configuration for RF sources was developed by Charles Spindt *et al.* at SRI International and is referred to as the Spindt Cathode [38]. Spindt cathodes consist of microfabricated metal field emitter cones deposited on a conducting base by a thin film deposition process. Each emitter has its own concentric aperture in an accelerating field generated by a gate electrode, which is isolated from the emitter/base by a silicon dioxide insulator. The configuration is illustrated in Fig. 9. The FEA is created by simultaneously depositing the cone and a liftoff material in etched cavities that are continually rotated during the process. The process is illustrated in Fig. 10. Variations in the process can produce a number of different configurations with special properties. Packing densities exceeding $10^8/\mathrm{cm^2}$ are achievable. With individual tips capable of producing hundreds of microamps, large arrays can theoretically produce very large emission densities. Current densities in excess of 2400 $\mathrm{A/cm^2}$ have been reported [42]. Fig. 11 shows scanning electron micrographs of an FEA and cross section of a single emitter.

The cathode can be operated emission-gated, where the electron beam is turned on and off using the gate voltage. At frequencies below 10 GHz, this can provide the axial bunching necessary to produce RF power. As the frequency increases, however, the capacitance between the base/emitters and gate becomes a limiting factor.

Design of electron guns is considerably simplified with cathodes that operate at room temperature. The guns operate instantly without requiring warm-up, as for thermionic cathodes, so they are ideal for fast turn on applications. Detailed thermal analysis of the mechanical structure to ensure proper positioning of electrodes at operating temperature can also be eliminated. There is no heater power supply, though a gate power supply is required. This supply requires considerably less power than typical heater power supplies.

A number of issues must be addressed before FEAs can be routinely implemented in typical vacuum electron devices. FEAs can work quite nicely in devices with very low vacuum pressures when operated at low beam voltages. Most high-power RF sources, however, do not operate in these regimes. FEAs are easily contaminated by adsorption of background gases and material sputtered off surfaces by electron impact or from backstreaming ions created by electron impact of background gases. They are especially susceptible to destruction from electrical arcs. While improvements in the design allow some protection and recovery for emitter to gate arcs, arcs from the anode or intermediate electrodes to the gate or emitter usually result in total cathode destruction. Because electrical arcs are typical during processing of most vacuum electron RF sources, this represents a serious problem. Other issues arise due to nonuniform emission from the emitter

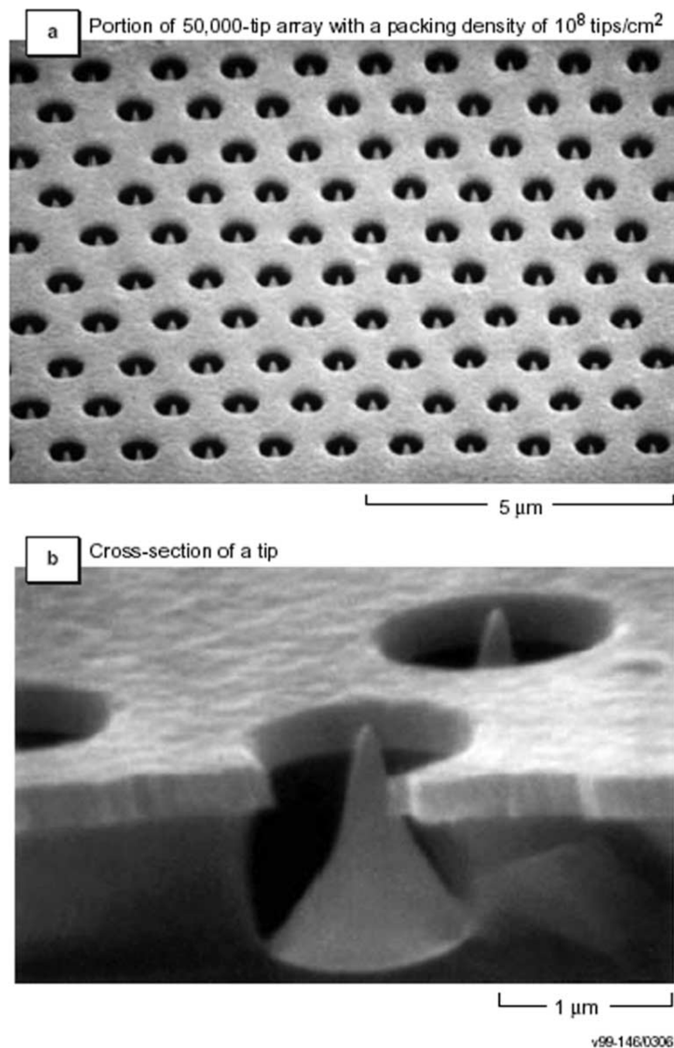

Fig. 11. FEA showing a portion of a 50 000 tip array. There is a 2-μm spacing between tips. Lower image is a cross section of a single emitter. (Reproduced from *Vacuum Microelectronics*, W. Zhu, Ed. New York: Wiley, 2000).

tips. While high current densities are achievable from single or small emitter arrays, it becomes increasingly difficult for larger arrays. Maximum current density achieved at CCR with a 1-mm-diameter array is less than 10 $\mathrm{A/cm^2}$. It is anticipated that current densities in excess of 100 $\mathrm{A/cm^2}$ will be obtained from an array with a 400-μm diameter [43]. An excellent review article on FEAs was published by Nation *et al.* in 1996 [44]. This article describes the detailed characteristics of FEAs, the emission physics, and applications.

Makishima *et al.* at NEC reported operation of a traveling wave tube using a Spindt-type field emitter at X band in 1997 [45]. The device achieved 27.5 W at 10.5 GHz with a gain of 19.5 dB, voltage of 3.35 kV, and cathode current of 58.6 mA. The efficiency was 14%; however, the beam transmission was only 82%. A later version corrected the beam transmission problem, achieving 99.3% transmission [46]. This device operated at 11.5 GHz and generated 28.2 W with 10% efficiency.

Whaley *et al.* at Northrop Grumman in Rolling Meadows, IL (now L-3 Communications, Inc.) implemented an FEA cathode in a TWT operating from 3.9 to 6.75 GHz with 100-ms pulses [47]. Axial bunching of the electron beam was achieved by modulating the gate voltage. The operating voltage was 3.2 kV, and the TWT produced a maximum output power of 280 mW. The cathode current density was approximately 7 $\mathrm{A/cm^2}$. More recent results using ungated cathodes demonstrated operation at 10 $\mathrm{A/cm^2}$ with 99.5% beam transmission. This device produced 55 W at 4.5 GHz with 17% efficiency. Experiments are under way to investigate degradations in performance with time [48]. The TWT was operated at 35 mA, 1% duty for 175 h with no significant degradation in cathode emission. Additional life tests are in progress.

Interest in FEAs for RF sources increased dramatically in the last year. Since Spring 2002, CCR has received three programs to investigate implementation of FEAs in RF devices. The U.S. Air Force is supporting development of a W band TWT for satellite communications [49], [50]. The program is funding development of an electron gun producing a 200 μm diameter electron beam delivering 28 mA at 9.0 kV. In order to avoid beam compression in the electron gun, the cathode must operate at 90 $\mathrm{A/cm^2}$, which should be within the capability of existing FEAs. The U.S. Air Force is also funding an FEA improvement program focused on implementation into RF sources. The program will examine FEA geometry, manufacturing techniques, and processes to reduce susceptibility to high-voltage cathode to anode arcs and back ion bombardment, and to improve emission uniformity in large arrays [51]. CCR is teamed with SRI International in this research. The FEA test device shown in Fig. 12 allows testing of FEAs up to 100 kV. The U.S. Army is funding development of miniature TWTs for phased array antennas at Ka band. The goal is to utilize FEA cathodes producing a 300-μm diameter electron beam with a current emission density approaching 100 $\mathrm{A/cm^2}$. The U.S. Air Force will be funding a new Multidisciplinary University Research Initiative program focused on development of field emitters for RF sources [52].

B. Circuits

Because the size of most circuits is inversely proportional to frequency, manufacture, and assembly for higher frequency devices becomes problematic. Few fundamental devices are in production above V band, as traditional machining techniques cannot achieve the tolerances required. As the frequency increases, the research focuses on circuits that can be manufactured in planar geometries suitable for lithographic or wire EDM technologies. Devices include klystrons, TWTs, BWO, and Smith–Purcell devices.

1) W Band Klystrino: One of the first vacuum electron devices built using lithographic techniques was the klystrino designed at Stanford Linear Accelerator Center (SLAC) [8]. Schietrum *et al.* used LIGA to generate the circuit for the W band device. A photograph of the circuit is shown in Fig. 13. The device was designed to produce 100 kW of power at 95 GHz. The circuit is shown on the right side and contains six cavities, including a five gap output cavity. The beam tunnel was cut using wire EDM. LIGA was selected because of the high surface finish that could be achieved.

This was a major accomplishment in microfabrication, as it was one of the first to demonstrate the application of LIGA for this class of device. It also demonstrated that electroplated

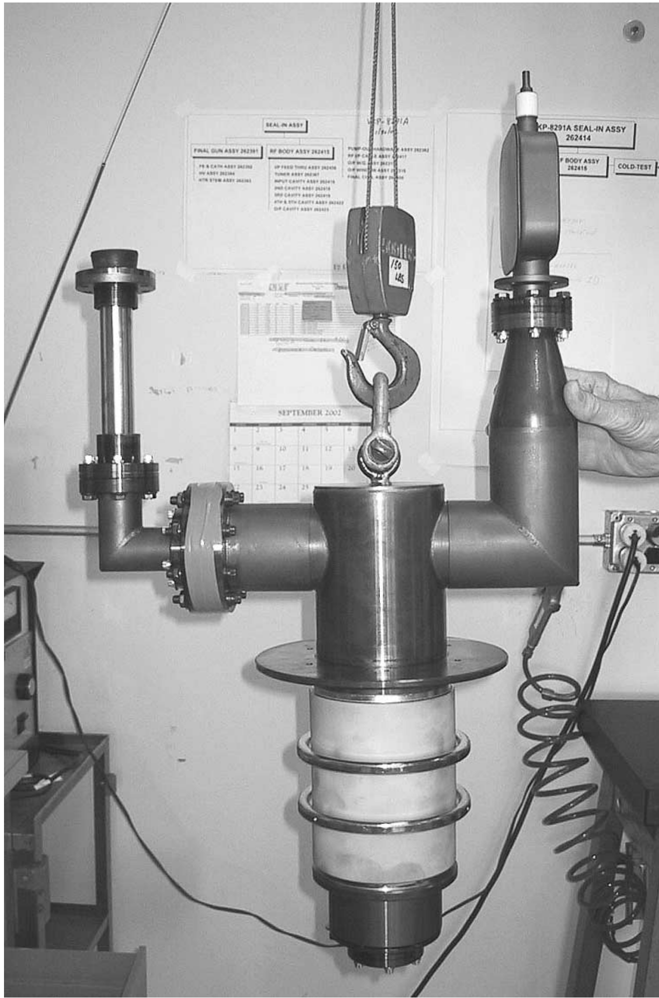

Fig. 12. Experimental device for high-voltage testing of field emission array cathodes.

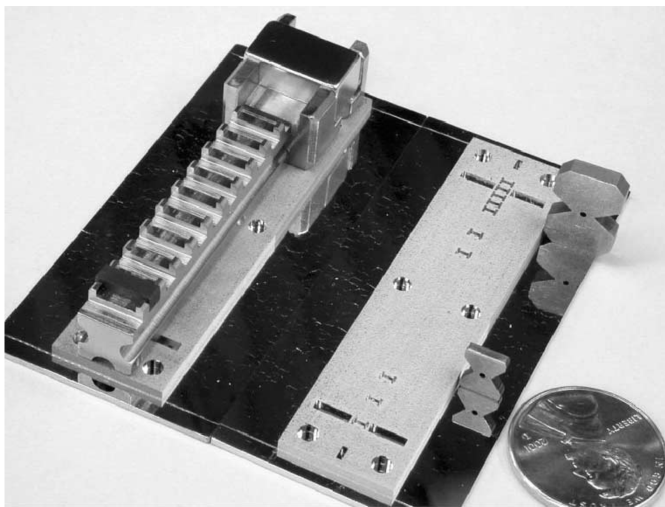

Fig. 13. W band klystrino built at Stanford Linear Accelerator Center.

copper structures generated in the LIGA process were sufficiently robust to withstand braze and bakeout temperatures. Unfortunately, a magnetics problem generated a beam misalignment during initial testing that destroyed the output structure.

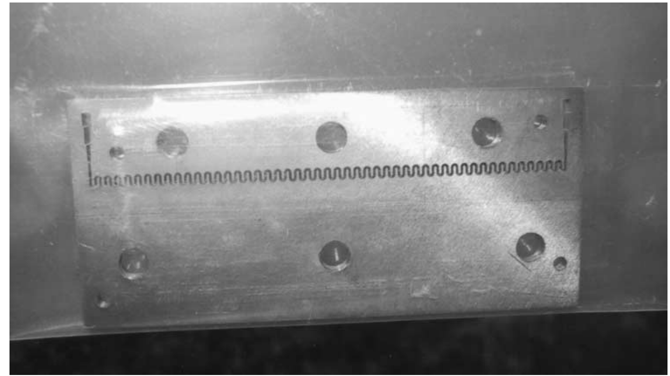

Fig. 14. 83.5-GHz folded waveguide circuit with input and output couplers.

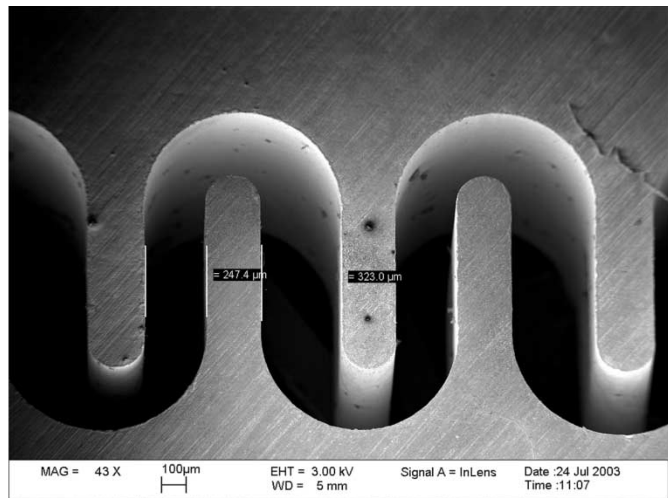

Fig. 15. Microphotograph of a section of the 83.5-GHz folded waveguide circuit structure.

2) W Band TWT: CCR is developing folded waveguide circuit structures for TWTs at Ka band and W band. The folded waveguide structure is planar and allows the input and output couplers to be included in the machining process. Initially, it was planned to use both LIGA and EDM technologies to produce these circuits; however, the results from EDM were so encouraging that it was selected by the funding agency for the primary approach. A folded waveguide test structure is shown in Fig. 14. The circuit period is 1060 μm, and the waveguide slot is 297 μm wide. The input and output couplers were designed using the optimization capability of CASCADE to transition to standard W band waveguide.

A 626-μm diameter beam tunnel was inserted through the circuit using plunge and wire EDM. First, smaller diameter holes were punched through from each end and met in the center. Then, an EDM wire was threaded through the holes and used to generate the final 626-μm diameter beam tunnel.

A microphotograph of the folded waveguide test structure of Fig. 14 is shown in Fig. 15. The asymmetry in the radial structures resulted from a misalignment during manufacture and was accurately reproduced over the entire circuit length. Note the high surface finish inside the waveguide. The circuit shown in Fig. 14 was integrated into an assembly for testing at the University of Wisconsin-Madison. The results will be used to quantify

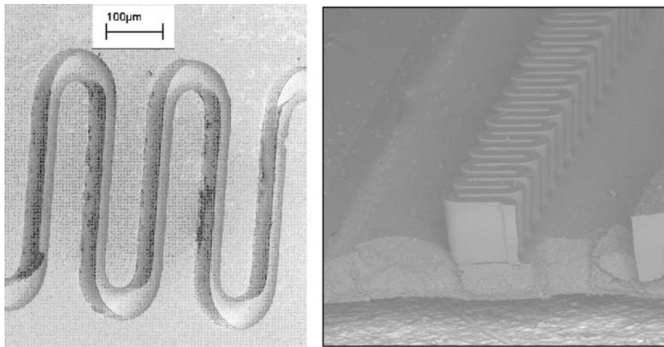

Fig. 16. 400-GHz folded waveguide traveling wave tube circuit structures produced by deep reactive ion etching (left) and UV-LIGA with SU-8 (right).

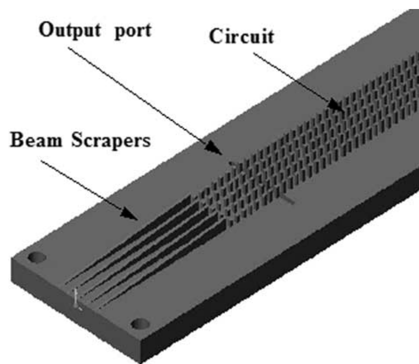

Fig. 17. Front end of 600–700 GHz BWO circuit, showing beam scraper and output coupling port.

the quality of the surface finish and the accuracy of computer simulations.

3) 400-GHz TWT: Booske *et al.* are exploring folded waveguide circuits in the submillimeter range [53]. The photograph shown in Fig. 2 was a folded waveguide circuit at approximately 400 GHz using LIGA. Fig. 16 shows similar circuit structures generated using DRIE and SU-8. The left image is a circuit structure etched into silicon, and the right image shows a negative image of a circuit. While these demonstrate capability to generate relevant structures, neither represents a usable circuit for an RF device, and additional research is in progress.

4) 600–700 GHz BWO: Fig. 17 shows the front end of a 600–700 GHz backward wave oscillator circuit under development for the National Aeronautics and Space Administration [54]. The circuit consists of five parallel slow wave structures made up of metal posts, or pintles, that are 20×20 μm in cross section and 80 μm high. Each circuit consists of 300 pintles, resulting in a total of 1500 features. A rectangular electron beam emitted by a thermionic cathode passes above and between the five slow wave structures. The bandwidth is approximately 15% and the device will produce 6–8 mW of RF power.

This circuit requires 3-D structures in an otherwise planar circuit. The beam scrapers must be tapered to properly shape the electron beam, and the output port consists of a fundamental waveguide whose direction is perpendicular to the beam direction.

Both LIGA and EDM circuits are being investigated for this device. Sandia National Laboratories is developing LIGA circuits at several frequencies ranges up to 1.9 THz. Previous attempts to manufacture LIGA-generated circuits failed for various reasons. An initial problem occurred because of the copper substrate. Backscatter of the synchrotron radiation from the substrate exposed PMMA beneath the X-ray mask, destroying the fidelity of the features. This problem was overcome by reducing the energy of the radiation. Sandia was successful in creating the circuit structure in the PMMA and electrodepositing the copper to generate the features. Unfortunately, the PMMA released prematurely from the copper substrate, destroying the pintles. Interestingly enough, the pintles remained attached to the substrate despite significant shear forces. This provided optimism that the process could ultimately be successful, so another attempt was funded. To provide greater probability of success, the rectangular pintles were changed to cylindrical structures, and the beam shaver was reduced in length. Modifications were incorporated in the mask layout to reduce forces that would cause the PMMA to prematurely release from the substrate. This attempt was more successful, and a portion of the 600–700 GHz circuit is shown in Fig. 18. A closeup of this section was shown in Fig. 3.

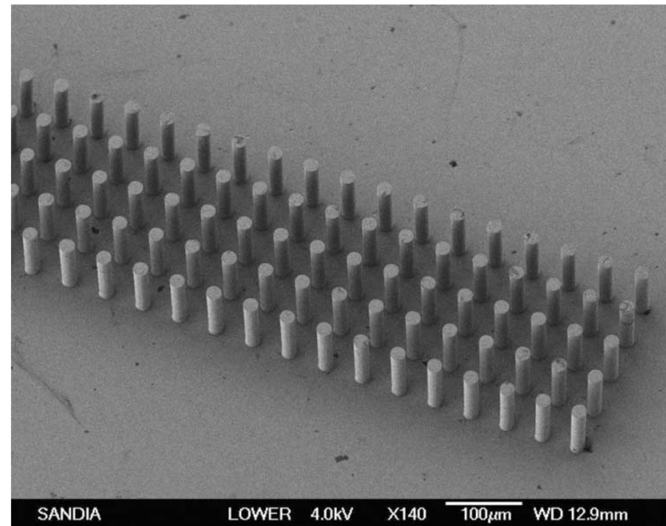

Fig. 18. Section of 600–700 GHz BWO circuit produced with LIGA. All features are copper. Periodicity of the pintles is 50 μm in the axial (left to right) direction. The pintles are 20 μm in diameter and 80 μm high.

Currently, EDM appears to be more appropriate for BWOs below 800–900 GHz. Recent implementation of 20 μm wire to cut the circuit structures allows slots to be cut approximately 80 μm deep and 25 μm wide. This implies that BWO circuits up to approximately 1 THz could be manufacturable using EDM. Recent development of EDM machines capable of handling 15-μm-diameter wire may extend this capability to higher frequencies [55]. For frequencies above 1 THz, only lithographic techniques provide potential manufacturing capability for the circuit. Even for lithographically produced circuits, however, significant EDM machining will be required to add the output waveguide, RF coupling features, and matching tapers.

EDM test structures of the BWO circuit were successfully cut, demonstrating capability to create the circuit. The difficulty comes in cutting the slots between the five circuit structures. This slot is 34 μm wide, 80 μm deep, and 1.2 cm long. Bending of the wire required construction of the circuit in two sections.

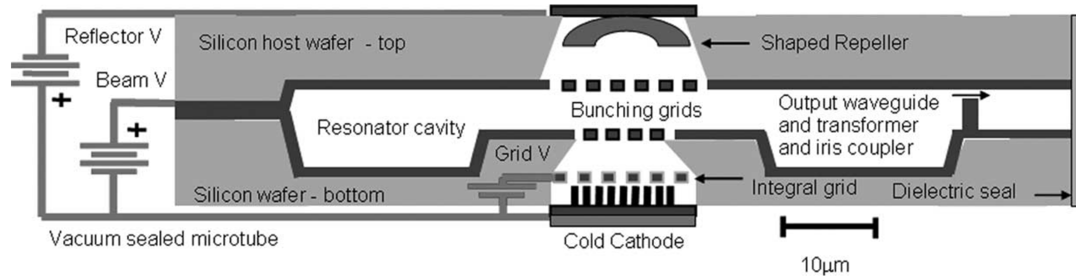

Fig. 19. Schematic of the reflex klystron. The cavity, beam tunnel, and output waveguide are etched from silicon wafers using deep reactive ion etching.

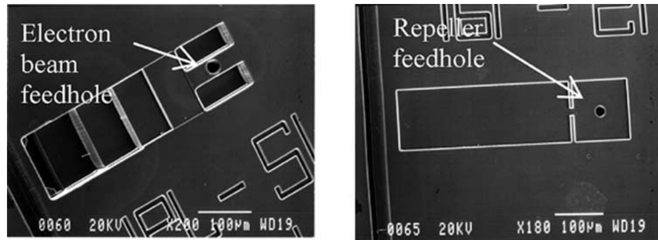

Fig. 20. SEM images of top and bottom halves of 1.2-THz nanoklystron.

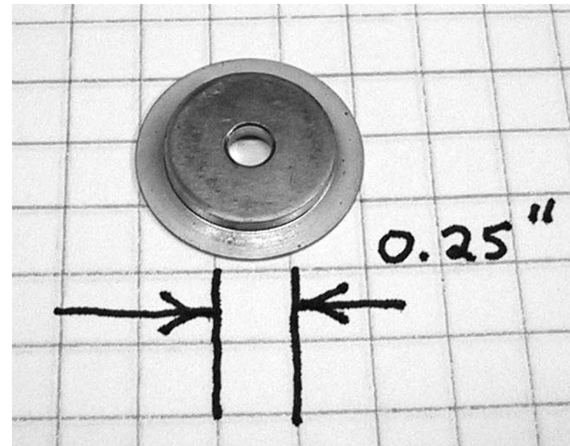

Fig. 21. Russian 100-μm-thick window.

This is still not a production operation, however. EDM machines are just becoming available to handle 20 μm and smaller wire. Issues of wire tension, synchronism of feed and takeup rollers, and arc energy continue to make manufacture of micrometer size structures a time consuming and tedious operation.

5) 1200-GHz Nanoklystron: Researchers at NASA's Jet Propulsion Laboratory are developing a 1200-GHz reflex klystron predicted to provide 3 mW of RF power [56]. The device consists of a high-current density cathode, bunching tube, RF resonator, shaped repeller, and RF output port, all fabricated monolithically on two bonded silicon wafers. Fig. 19 shows a schematic of the device. The cavity, beam passages, and output waveguide are etched from two silicon wafers using deep reactive ion etching, then bonded together. SEM photographs of the top and bottom sections are shown in Fig. 20. The top and bottom halves are coated with chromium, platinum, and gold layers using e-beam evaporation. The two wafers are aligned and bonded at 450 °C under high pressure. Apertures are etched in the top and bottom for the electron source and repeller. The devices will be tested in an ultrahigh-vacuum test chamber using a conventional thermionic cathode. It is anticipated that the thermionic cathode will be replaced with an ultrahigh-current density FEA source operating with an emission current density exceeding 1 $\mathrm{kA/cm^2}$.

6) RF Windows and Waveguides: Essentially all vacuum electron devices require vacuum windows to transmit RF signals into and out of the vacuum. Typically, these employ ceramic materials that are a multiple of a half wavelength thick with the desire to minimize the thickness to provide increased bandwidth. The power in lower frequency tubes is typically transmitted through alumina ceramic windows, which at centimeter frequencies are on the order of 1–5 mm thick. At 600 GHz, however, a half wavelength window is on the order of 70 μm thick. In this regime the structural integrity of materials and assembly techniques become especially critical. Pressed ceramic materials, for example, may crumble at these thickness, or the finite porosity may lead to vacuum leaks. One has to ensure the window can support the stresses from atmospheric pressure, in addition to those from RF power generation.

In the BWO described in Section IV, a number of factors forced a completely new approach to RF window design and assembly. The original BWOs manufactured by Istok Company used windows where molten glass was flowed over an aperture and allowed to solidify. This resulted in windows approximately 100 μm thick, though the window surfaces were not parallel or flat. One of these windows is shown in Fig. 21. Unfortunately, the quasi-optical design of the CCR BWO required a window thickness of 70 μm.

The first issue was determination of a window material. Several options were considered, including alumina, Boron nitrite, sapphire, and chemically vapor deposited (CVD) diamond. Concern for vacuum leaks from finite porosity led to elimination of all pressed and sintered ceramics, such as alumina. CVD diamond was considered, but there were concerns over cost and availability. Sapphire was readily available at the diameters required and was the most obvious choice due to its strength, thermal conductivity, low RF loss, and crystalline structure. Thermomechanical analysis indicated that it could adequately withstand the applied stresses from atmospheric pressure and the anticipated thermal power deposition. The analysis also indicated, however, that the material would fail catastrophically during brazing to any metallic sleeve, even dead soft copper.

A design was developed where a thick (3 mm) sapphire disk was brazed into a copper sleeve, which was then assembled into the window structure. The sapphire was then ground to

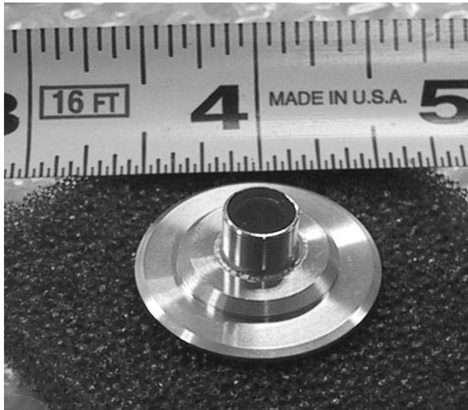

Fig. 22. 70-μm-thick sapphire BWO window.

the desired 70 μm thickness. This was not a trivial development, and numerous problems were overcome, including design of backing ceramic structures, braze fixturing, sapphire metallization, support of the sapphire against grinding stresses, and grinding speed and pressure. It required a concerted effort between window designers, mechanical engineers, brazing specialist, grinding specialist, and ceramics/sapphire vendors to develop a design and process that was successful. A completed window assembly is shown in Fig. 22. The window will be laser welded to the BWO body assembly.

The point here is that very few assembly issues are simple at millimeter and submillimeter frequencies. Materials, processes, and designs that work at S band or Ku band may be totally inadequate at higher frequencies. Even transmission in fundamental waveguide becomes a problem due to high RF losses. In many cases, it may be more advantageous to use quasi-optical modes or overmoded waveguide.

7) Magnetics: Most all RF sources propagating an electron beam require a magnetic field for focusing and beam propagation. For TWTs and some klystrons, this is traditionally accomplished with periodic permanent magnet (PPM) focusing consisting of a stack of alternating permanent magnets and iron disks through which the beam propagates. For lower frequency devices, it is possible to assemble these structures external to the vacuum envelope and adjust the field with shunts to compensate for asymmetries or minor misalignments. As the size of the RF circuit shrinks with increasing frequency, so do the required sizes of the magnetic circuit structures. Eventually, one reaches the point where the stack must be within the vacuum envelope to be sufficiently close to the beam. In this situation, there is no practical way to apply shunts to precisely align the fields. An example is the klystrino, shown in Fig. 13. Two of the magnetic circuit components are shown on the right side of the image with central holes for passage of the electron beam. In these cases, it is necessary to ensure that the magnetic field profile is correct before the device is completely assembled. This requires development of sufficiently uniform and repeatable permanent magnet structures or developing equipment to measure the axial and transverse field. An asymmetry in the magnetic field led to the destruction of the klystrino during test.

Equipment to measure magnetic fields, both axial and transverse, in millimeter or submillimeter linear devices will be challenging. The beam tunnel in the W band TWT described in Section II is approximately 3 cm long with a 400-μm diameter. The beam tunnel in the BWO described in Section IV is approximately 2 cm long with transverse dimensions of 100×600 μm.

It may be more practical to utilize a nonperiodic field produced by an external permanent magnet or solenoid. Depending on the application, however, this could be unacceptable. Space applications are very concerned about size, weight, and power. There is a strong emphasis to avoid additional power supplies for solenoids. External permanent magnets can be quite heavy. The permanent magnet for the 650-GHz BWO weighs approximately 30 kg and occupies 25 200 mm^3. The BWO itself weighs less than 100 g and occupies less than 360 mm^3.

IV. Additional Research Requirements

There are no production vacuum electron devices currently using lithographically produced components to produce RF power at high frequencies. A number of devices are in development, however, and it is certain that many of the current problems will be overcome. It is not clear that obstacles can be overcome for certain processes, and only additional research will resolve these issues. All lithographically produced components are still primarily laboratory structures.

For LIGA, it will be important to address synchrotron availability before this technique can be considered for production applications. For one of a kind or small quantity applications, it may be appropriate. There are still other issues that must be overcome before the process itself can be considered reliable. The problems demonstrated in Fig. 2, the difficulty manufacturing the 650-GHz BWO circuit, and the current six- to nine-month lead times are issues that one must consider before designing components using LIGA.

SU-8 seems to be dependent on a large number of parameters that are somewhat dependent on the particular device being produced. A persistent problem is stress fracturing. Researchers are working on more clearly defining the process, but there currently is no consensus. To the author, there still appears to be too much black magic in this process for it to be considered reliable or repeatable.

Deep reactive ion etching issues include scalloping and straightness of the side walls. It is also a process in silicon, so one must generate molds that can then be electroplated to form actual structures. Recent results are encouraging, so interested readers should follow developments closely.

EDM is currently producing parts for actual RF devices. The process is used for manufacturing grids for electron guns, and a recent W band gyroklystron used cavities manufactured by EDM [57]. A significant investment in equipment may be required, however, to produce large numbers of microfabricated components in a production environment.

FEAs could potentially revolutionize the RF industry by providing inexpensive, high current density, room temperature, electron sources with unlimited lifetime. Much additional development will be required to design FEAs that are reliable and sufficiently rugged for typical VED applications. Issues, such as arc protection, contamination, emission uniformity, high average power operation, and lifetime, must be addressed.

Innovative solutions are required to develop magnetic or electrostatic focusing schemes for beam propagation through microfabricated devices. This should include research into new materials, configurations, measurement and design techniques, processes, and equipment. Perhaps high-temperature superconductors or advances in cryogenics could provide solutions for some applications.

V. Conclusion

The demand for high-frequency RF sources is driving research on a new class of devices utilizing advanced microfabrication techniques and innovative structures. While significant progress has been achieved in laboratory environments, much additional work is required to transition these techniques and devices into a production environment. Success will require close cooperation between the RF source industry and universities and laboratories developing lithographic processes for fabrication of submillimeter and terahertz relevant structures. Potential applications for homeland security, communications, material studies, and basic research could provide significant return on investments in this area. This is an exciting new world for engineers and scientists that is renewing interest in the RF source and component industry.

References

[1] D. Woolard, R. Kaul, R. Suenram, A. H. Walker, T. Globus, and A. Samuels, "Terahertz electronics for chemical and biological warfare agent detection," in *IEEE MTT-S Dig.*, 1999, pp. 925–928.

[2] S. Wang, B. Ferguson, C. Mannella, D. Abbott, and X.-C. Zhang, "Powder detection using THz imaging," in *Tech. Dig. Summaries of Papers Presented at the Quantum Electronics and Laser Science Conf.*, Long Beach, CA, May 2002.

[3] S. W. Smye, J. M. Chamberlain, A. J. Fitzgerald, and E. Berry, "The interaction between terahertz radiation and biological tissue," *Phys. Med. Biol.*, vol. 46, pp. R101–R112, 2001.

[4] X.-C. Zhang, "Terahertz wave imaging: Horizons and hurdles," *Phys. Med. Biol.*, vol. 47, pp. 3667–3677, 2002.

[5] C. Kory, private communication, Jan. 2004.

[6] D. L. Rockwell, "SARs will remain budget stars," *Aerospace America*, 2002.

[7] U.S. Army Small Business Technology Transfer Research Grant DAAD19–03-C-0089.17.

[8] G. Scheitrum, G. Caryotakis, A. Haase, B. Arfin, C. Pearson, L. Song, N. Luhmann, B. James, B. Shew, and Y. Cheng, "95 GHz klystron design and fabrication," in *Multidisciplinary University Research Initiative Teleconf.*, Oct. 2000.

[9] R. Ruhmann, K. Pfeiffer, M. Falenski, F. Reuther, R. Engelke, and G. Grutzner, "SU-8—A high performance material for MEMS applications," *Polym. MEMS*, pp. 45–46, Jan. 2002.

[10] A. Nassiri, Y. W. Kang, and J. J. Song, "Millimeter-wave structures and drivers for future linear colliders," in *25th Int. Conf. Infrared and Millimeter Waves*, Beijing, China, Sept. 2000.

[11] J. J. Song, S. Bajikar, F. Decarlo, Y. W. Kang, R. L. Kustom, D. C. Mancini, A. Nassiri, B. Lai, A. D. Feineman, and V. White, "LIGA-fabricated compact mm-wave linear accelerator cavities," *Microsyst. Technol.*, vol. 4, pp. 193–195, 1998.

[12] W. Ehrfeld, M. Abraham, U. Ehrfeid, M. Lacher, and H. Lehr, "Materials for LIGA products," in *Proc. IEEE Micro Electro Mechanical Systems. An Investigation of Micro Structures, Sensors, Actuators, Machines and Robotic Systems*, Oiso, Japan, Jan. 1994, pp. 86–90.

[13] J. J. Song, S. Bajikur, Y. W. Kang, R. L. Kustom, D. C. Mancini, A. Nassiri, and B. Lai, "LIGA fabrication of mm-wave accelerating cavity structures at the advanced photon source," in *Proc. 1997 Particle Accelerator Conf.*, vol. 1, Vancouver, BC, Canada, May 1997, pp. 461–463.

[14] R. Merte, H. Henke, and R. Apel, "Design, fabrication, and RF measurement of a W-band accelerating structure," in *Proc. 1999 Particle Accelerator Conf.*, New York, 1999, pp. 818–820.

[15] J. Booske and University of Wisconsin-Madison, private communication, July 2003.

[16] V. Saile, "Strategies for LIGA implementation," in *Micro Systems Technologies 98. 6th Int. Conf. Micro Electro, Opto, Mechanical Systems and Components*, Potsdam, Germany, Dec. 1998, pp. 25–30.

[17] J. Gelorme, R. J. Cox, and S. A. R. Gutierrez, "Photoresist composition and printed circuit boards with packages made therewith," U.S. Patent 4 882 245, Nov. 21, 1989.

[18] L. Jingquan, Z. Jun, D. Guipu, A. Xiaolin, and C. Bingehu, "Orthogonal method for processing of SU-8 resist in UV-LIGA," in *Micromachining and Microfabrication Process Technology*, 2001, vol. 4557, Proc. SPIE, pp. 462–466.

[19] K. Lian, Z.-g Ling, and C. Liu, "Thermal stability of SU-8 fabricated microstructures as a function of photo initiator and exposure doses," in *Reliability, Testing, and Characterization of MEMS/MOEMS II*, R. Ramesham and D. M. Tanner, Eds., 2003, vol. 4980, Proc. SPIE, pp. 208–212.

[20] L. Singleton, A. L. Bogdonov, S. S. Peredkov, O. Wihelmi, A. Schneider, Carstn, Cremers, S. Megtert, and A. Schmidt, "Deep x-ray lithography with the SU-8 resist," in *Emerging Lithographic Technologies*, V. Elizabeth and A. Dobiasz, Eds., 2001, vol. 4343, Proc. SPIE, pp. 182–192.

[21] D. W. Johnson, A. Jeffries, D. W. Minsek, and R. J. Hurditch, "Improving the process capability of SU-8. Part II," *J. Photopolymer Sci. Technol.*, vol. 14, no. 5, pp. 689–694, 2001.

[22] G. J. O'Brien, D. J. Monk, and K. Najafi, "Sub-micron high aspect ratio silicon beam etch," in *Device and Process Technologies for MEMS and Microelectronics II*, J.-C. Chiao, Ed., 2001, vol. 4592, Proc. SPIE, pp. 315–325.

[23] J. Bhardwaj, J. Ashraf, and A. McQuarrie, "Dry silicon etching for MEMS," in *Symp. Microstructures and Microfabricated Systems, Electrochemical Soc.*, 1997.

[24] E. H. Klassen, K. Petersen, J. M. Noworolski, J. Logan, N. I. Maluf, J. Brown, C. Storment, W. McCulley, and G. T. Kovacs, "Silicon fusion bonding and deep reactive ion etching: A new technology for microstructures," *Sens. Actuators A*, vol. 52, pp. 132–139, 1996.

[25] P.-A. Clerc, L. Dellmann, F. Gretillat, M.-A. Gretillat, P.-F. Indermuhle, S. Jeanneret, P. Luginbuhl, C. Marxer, T. L. Pfeffer, G.-A. Racine, S. Roth, U. Staufer, C. Stebler, P. Thlebaud, and N. F. de Roolj, "Advanced deep reactive ion etching: A versatile tool for microelectromechanical systems," *J. Micromech. Microend.*, vol. 8, pp. 272–278, 1998.

[26] J. Booske and Univ. Wisconsin-Madison, private communication, July 2003.

[27] (2001, Sept.). [Online]. Available: http://www.mmsonline.com/articles/099702.html

[28] D. Birk. EDM: Principles of Operation. [Online]. Available: www.edmtt.com/images/principles.pdf

[29] ——, (2000) Different types of machining processes that use EDM. [Online]. Available: www.edmtt.com/articlereports/edmprocesses.html

[30] S. Schwartzkopf, private communication, Jan. 2003.

[31] R. Forster, A. Schoth, and W. Menz, "Micro-Wire-EDM for production of microsystems in steel and ceramics," in *High Aspect Ratio Micro-Machining Technology Workshop*, Monterey, CA, June 2003.

[32] J. M. Neilson, "An improved multimode horn for Gaussian mode generation at millimeter and submillimeter wavelengths," *IEEE Trans. Antennas Propagat.*, vol. 50, pp. 1077–1081, Aug. 2002.

[33] T. Gmelin, H. Kuck, M. Kock, and R. Schuster, "High aspect ratio ultra precise machining of stainless steel by electrochemical milling with ultra short pulses," in *High Aspect Ratio Micro-Machining Technology Workshop*, Monterey, CA, June 2003.

[34] American Precision Dicing. [Online]. Available: http:///www.waferdicing.com/materials.htm

[35] M. Mross, private communication, Sept. 2003.

[36] J. Walsh, "Grating Coupled Free Electron Laser Apparatus and Method," U.S. Patent 5 790 585, 1998.

[37] M. Mross, T. H. Lowell, R. Durant, and M. F. Kimmitt, "Performance characteristics of a Smith-Purcell tunable terahertz source," *J. Biol. Phys.*, vol. 29, pp. 295–302, Jan. 2003.

[38] C. A. Spindt, I. Brodie, C. E. Holland, and P. R. Schwoebel, "Spindt field emitter arrays," in *Vacuum Microelectronics*, W. Zhu, Ed: Wiley, 2001.

[39] R. Shuman, K. Noll, and D. Casey, Jr., "Method and Apparatus for Milling Copper Interconnect in Charged Particle Beam System," U.S. Patent 6 322 672, Nov. 2001.

[40] D. Casey, M. Phaneuf, C. Chandler, M. Megorden, K. Noll, R. Schuman, T. Gannon, A. Krechmer, D. Monforte, N. Antoniou, N. Bassom, J. Li, P. Carleson, and C. Huynh, "Copper device editing: Strategy for focused ion beam milling of copper," *J. Vac. Sci. Technol. B*, vol. 20, pp. 2682–2685, Nov./Dec. 2002.

[41] B. Li, X. Tang, H. Xie, and X. Zhang, "Focused ion beam (FIB) nanomachining and FIB moire technique for strain analysis in MEMS/NEMS structures and devices," in *Proc. IEEE 16th Int. Conf. Micro Electro Mechanical Systems*, Jan. 2003, pp. 674–677.

[42] L. Parameswaran, R. A. Murphy, C. T. Harris, R. H. Matjheows, C. C. Graves, M. A. Hollis, J. Shaw, M. A. Kodis, M. Garven, M. T. Ngo, K. L. Jenwsen, M. Green, J. Legarra, L. Garbini, and S. Bandy, "Field emitter arrays for inductive output amplifiers," in *Vacuum Electronics Annu. Rev. Abstracts*, San Diego, CA, May 1997, p. IV-7.

[43] C. Spindt, private communication, July 2003.

[44] J. A. Nation, L. Schachter, F. M. Mako, L. K. Len, W. Peter, C. M. Tang, and T. Srinivasan-Rao, "Advances in cold cathode physics and technology," *Proc. IEEE*, vol. 87, pp. 865–88, May 1999.

[45] H. Makishima, H. Imura, M. Takahashi, H. Fukui, and A. Okamoto, "Remarkable improvements of microwave electron tubes through development of the cathode materials," in *Tech. Dig. Int. Vacuum Microelectronics Conf.*, Kyongju, Korea, 1997.

[46] H. Makishima, S. Miyano, H. Imura, J. Matsuoka, H. Takemura, and A. Okamoto, *Appl. Surf. Sci.*, vol. 146, p. 230, 1999.

[47] D. R. Whaley, B. Gannon, V. O. Heinen, K. E. Kreischer, C. E. Holland, and C. A. Spindt, "Experimental demonstration of an emission-gated traveling wave tube amplifier," *IEEE Trans. Plasma Sci. (Special Issue on High Power Microwaves)*, vol. 30, pp. 998–1008, June 2002.

[48] D. R. Whaley, "Chapter contribution on cold cathode technology," *Innov. Vac. Electron.*, submitted for publication.

[49] "U.S. Air Force Small Business Innovation Research Grant F29601–03-C-0049," Kirtland Air Force Base, New Mexico.

[50] M. Read, R. L. Ives, C. Kory, and G. Miram, "MEMS-based TWT development," in *Int. Vacuum Electronics Conf.*, Seoul, Korea, May 2003.

[51] "U.S. Air Force Small Business Innovation Research Grant F33615–03-M-1509," Wright Patterson Air Force Base, Ohio, 2003.

[52] R. Barker, private communication, Apr. 2003.

[53] J. Booske, private communication, Mar. 2003.

[54] R. L. Ives, C. Kory, M. Read, J. Neilson, M. Caplan, N. Chubun, S. Schwartzkopf, and R. Witherspoon, "Development of a backward-wave-oscillator for terahertz applications," in *Terahertz for Military Applications*, vol. 5070. Orlando, FL, Apr. 2003, pp. 71–82.

[55] R. Witherspoon, private communication, July 2003.

[56] H. M. Manohara, P. H. Seigel, C. Marrese, B. Chang, and J. Xu, *Design and Fabrication of a THz Nanoklystron*: California Inst. Technol., Jet Propulsion Lab., 2003.

[57] W. Lawson, R. L. Ives, M. Mizuhara, J. M. Neilson, and M. E. Read, "Design of a 10-MW, 91.4-GHz frequency-doubling gyroklystron for advanced accelerator applications," *IEEE Trans. Plasma Sci.*, vol. 29, pp. 545–558, June 2001.

R. Lawrence Ives (S'83–M'83–SM'93) received the Ph.D. degree in plasma physics from North Carolina State University, Raleigh.

He began his microwave career in the Gyrotron Department at Varian Associates, Inc., Palo Alto, CA. In that position, he was responsible for designing electron guns, gyrotron circuits, collectors, and waveguide components. Gyrotrons are high power, high-frequency microwave and millimeter wave RF sources used for fusion research and industrial heating. He founded Calabazas Creek Research, Inc., which is involved in software development, microwave tube and component design, and uses of microwave power for environmental and heating applications. He was principle investigator in programs to develop a two-stage depressed collector system for Gaussian-mode gyrotrons at the 1-MW CW power level, S band multiple beam electron gun for radar applications, a MW CW waterload for Gaussian mode gyrotrons, and a 15-kW CW L band klystron for driving superconductor accelerator cavities. He is currently principle investigator on programs to implement field emission array cathodes into RF sources, multiple beam electron guns for high-power RF applications, improved magnetron injection guns for high power gyrotrons and gyroklystrons, a 50-MW multiple beam klystron, a microfabricated W band traveling wave tube for satellite communications, and terahertz backward wave oscillators. He also provides consulting support to several commercial companies on electron gun and RF source development.